

Embedded Large Eddy Simulation of Flow around a High-Rise Building with an Adjacent Structure

Xinyang Yu¹, Teng Wu²

¹ School of Civil Engineering, Central South University, Changsha, China,
xinyangyu@csu.edu.cn

² Department of Civil, Structural and Environmental Engineering, University at Buffalo, Buffalo, USA, *tengwu@buffalo.edu*

SUMMARY:

The embedded large eddy simulation (ELES) is a zonal hybrid method that offers potential for gains in computational efficiency by restricting the large eddy simulation (LES) to a specific portion of the computational domain while performing the Reynolds-averaged Navier-Stokes (RANS) simulation elsewhere. To evaluate its performance in complex wind environment of urban areas, the flow around a high-rise building with an adjacent structure is simulated by ELES in this work. The considered numerical model is comprised of two buildings, namely the principal building with an aspect ratio of 1:1:4 and the interfering building with an aspect ratio of 1:1:2. Results obtained from ELES are evaluated by available wind tunnel measurements. Comparisons suggest that ELES provides realistic representations of the flow fields and generates accurate wind pressure around the principal building.

Keywords: Computational Fluid Dynamics, Embedded Large Eddy Simulation, High-Rise Building

1. INTRODUCTION

High-rise buildings are very sensitive to wind loads, causing serious safety distress and posing significant serviceability issues. Compared to wind tunnel tests, the computational fluid dynamics (CFD) simulations provide high resolution flow fields at relatively low cost, making it another important way to investigate aerodynamic characteristics of structures. Among various CFD schemes, the Reynolds-averaged Navier-Stokes (RANS) simulation is popularly utilized due to its high computational efficiency. However, the simulation accuracy of RANS needs to be further improved, especially for root-mean-square (RMS) and peak wind loads. While the large eddy simulation (LES) is undoubtedly superior to RANS in terms of accuracy, but its applications are typically limited to moderate Reynolds numbers due to the mesh requirement in near wall regions. Hybrid LES/RANS approaches have been developed to balance the accuracy and efficiency. Different from the global hybrid models like detached eddy simulation (DES) and its variants, the embedded large eddy simulation (ELES) is a zonal hybrid method intended to combine the advantages of the accurate time-resolved solution of LES in the area near the structures of interest with the fast time-averaged solution of RANS in the far field. In this work, the accuracy and efficiency of ELES in modeling of the flow velocity and pressure fields around a high-rise building with an adjacent structure is evaluated, highlighting the aerodynamic

interference effects in the complex wind environment of urban areas. Comparisons of the ELES-based simulations and wind tunnel measurements suggest the good performance of ELES.

2. METHODOLOGY

The computational domain of ELES is typically split into RANS and LES zones, and the turbulence model is switched from RANS to LES on the interface with the synthetic turbulence for maintaining consistency.

2.1. LES and RANS Schemes

The calculations for RANS and LES zones are accomplished by respectively applying the ensemble averaging of and a low-pass filter to the governing equations. To keep the equations closure, the WALL Adaptive Local Eddy (WALE) viscosity model (Nicoud and Ducros, 1999) is adopted for the subgrid scale (SGS) stress modeling in LES scheme, and the realizable $k - \epsilon$ model (Shih et al., 1994) is adopted for the Reynolds stress modeling in RANS scheme.

2.2. Interface between LES and RANS Zones

2.2.1 RANS-LES interface

The LES zone is entirely engulfed in the RANS zone in this work. For the lateral and outflow boundaries of LES zone, the RANS quantities are directly used for simplicity. For the inflow boundary of LES zone, the generation of explicitly resolved turbulent eddies is required to provide unsteady fluctuations at the inlets. To construct time-dependent inlet conditions, the vortex method is utilized which generates small-scale turbulent motions by adding perturbations to the mean flow via a fluctuating two-dimensional vorticity field (Mathey et al., 2006).

2.2.2 LES-RANS interface

The mean flow data needs to be recovered from the resolved turbulent data in LES zone at the LES-RANS interface before reverting back to the RANS zone. While the mean flow data can be directly obtained by the unsteady LES data, the turbulent variables (including turbulent viscosity, turbulent kinetic energy and turbulent dissipation rate) are missing. A simple two-stage treatment for LES-RANS interface introduced by Gritskevich et al. (2016) is adopted in this study for the efficiency consideration. First, the flow is computed entirely by RANS model. Then, the RANS solution for turbulent variables is frozen within the LES zone and kept in the background during the LES computation. At the LES-RANS interface, the frozen solution from RANS model is reactivated, resolved turbulence structures from LES zone are allowed to pass into RANS zone.

3. COMPUTATIONAL SETTINGS

3.1. Computational Domain and Mesh Settings

The computational domain extends $15H \times 12H \times 6H$ in the streamwise (x), lateral (y), and vertical (z) directions, respectively, and LES region extends $3.25H \times 2.25H \times 3H$ in the x , y and z directions, as shown in Fig. 1. The domain is discretized by structured meshes. There are around 15 rows of cells in the boundary layer region of the principal building, and the distance of the first grid layer to the building surface is $5 \times 10^{-5}H$ with a cell expansion ratio of 1.05. More than 99.5% of wall cells present y^+ values of less than 1 with only a few exceptions in the range of $1 \leq y^+ < 4$. In the vertical direction, the grids are refined adjacent to the ground and the building top with a first cell height of $2 \times 10^{-4}H$ while expanded towards the middle with an expansion

ratio of 1.20. Away from the building, the cell size grows gradually to the maximum $0.05H$ within the LES region, and then to maximum $0.3H$ in the RANS region. The grids of two zones adjacent to the interfaces are designed to be similar size to minimize the effect of disparity of cell size on the flow stability when crossing the interface. Grid-dependency studies are conducted to choose the final computational grids with 3.28×10^6 cells.

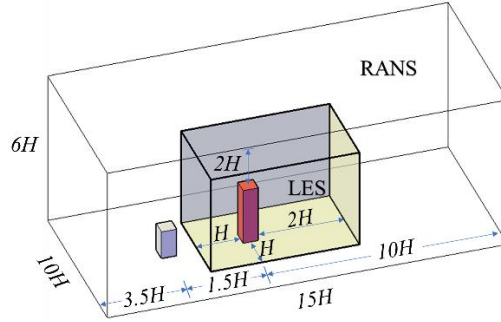


Figure 1. Computation domain.

3.2. Boundary Conditions and Numerical Schemes

The profiles of mean velocity and turbulence intensity used in the experiments performed by Tokyo Polytechnic University (Tamura, 2012) are applied as inlet conditions for a convenient validation. The Neumann and Dirichlet pressure conditions are respectively imposed at the inlet and outlet. The boundary conditions of upper and lateral surfaces are defined as slip wall while the boundary condition of building and the lower surfaces are set as non-slip wall. The simulation is carried out in ANSYS-FLUENT 19.0, unsteady ELES simulation is carried out based on the initial steady RANS realizable $k - \varepsilon$ simulation in the entire domain. Adopted numerical schemes are shown in Table 1.

Table 1. Numerical scheme.

Item	Scheme
Center to faces	Second-order bounded central difference
Convection term	third-order Quadratic Upstream Interpolation of Convective Kinematics (QUICK)
Diffusive term	Second-order central difference
Temporal	Bounded second-order implicit
Pressure-velocity coupling	Semi-Implicit Method for Pressure-Linked Equations Consistent (SIMPLEC)

4. RESULTS

Figure 2 presents the horseshoe vortex and wake vortex structures by means of iso-surfaces of the Q-criterion, indicating the simulated flow fields by ELES consistent with prior knowledge (Martinuzzi and Havel, 2000). As shown in Fig. 3, the streamlines structures suggest the existing of interfering building weaken the flow velocity near the sideways of principal building and induce reattachments in the sideways of principal building. The red line indicates the recirculation regions, which splitted by the reattachment in the sideways. The contour distribution of mean pressure coefficient $C_{p_{mean}}$ and RMS pressure coefficient $C_{p_{RMS}}$ are compared with the experimental measurements as shown in Fig. 4. The mean pressure coefficient is in good agreement with experimental results, and the RMS pressure coefficient is also generally consistent with experimental results (except some slight underestimations for the pressure coefficient of the windward).

REFERENCES

- Gritskevich, M.S., Garbaruk, A.V. and Menter, F.R., 2016, November. Investigation of the passage between LES and RANS subdomains in the framework of zonal RANS-LES approaches. In Journal of Physics: Conference Series (Vol. 769, No. 1, p. 012080). IOP Publishing.
- Mathey, F., Cokljat, D., Bertoglio, J.P. and Sergent, E., 2006. Assessment of the vortex method for large eddy simulation inlet conditions. Progress in Computational Fluid Dynamics, An International Journal, 6(1-3), pp.58-67.
- Martinuzzi, R.J. and Havel, B., 2000. Turbulent flow around two interfering surface-mounted cubic obstacles in tandem arrangement. J. Fluids Eng., 122(1), pp.24-31.
- Nicoud, F. and Ducros, F., 1999. Subgrid-scale stress modelling based on the square of the velocity gradient tensor. Flow, turbulence and Combustion, 62(3), pp.183-200.
- Shih, T.H., Liou, W.W., Shabbir, A., Yang, Z. and Zhu, J., 1994. A new k-epsilon eddy viscosity model for high Reynolds number turbulent flows: Model development and validation (No. CMOTT-94-6).
- Tamura, Y., 2012. Aerodynamic database for low-rise buildings. Tokyo Polytech. Univ <http://wind.arch.t-kougei.ac.jp/system/eng/contents/code/tpu> last accessed.

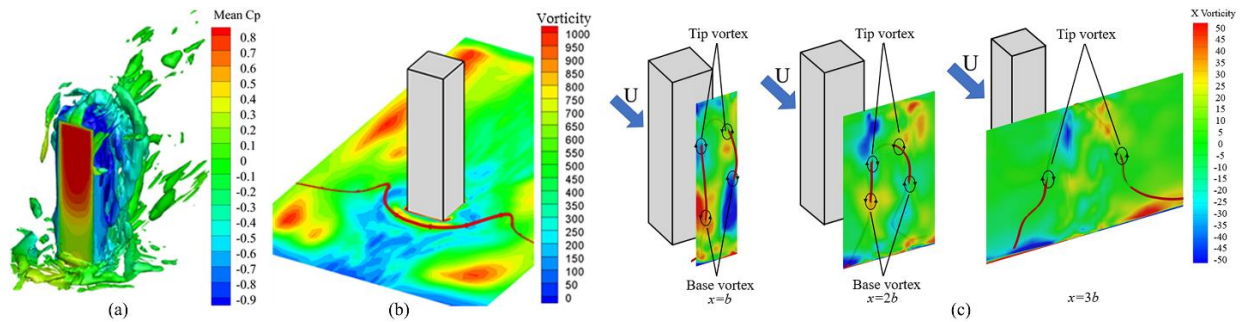


Figure 2. Vortex structures. (a) transient horseshoe vortex ($Q = 20,000s^{-2}$), (b) averaged horseshoe vortex, (c) wake vortex structure of plane at $x = b$, $x = 2b$, $x = 3b$.

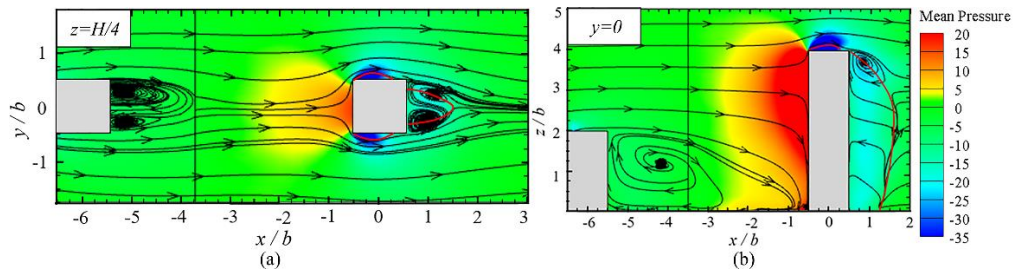


Figure 3. Mean streamline structures. (a) plane at $z = h/4$, (b) plane at $y = 0$.

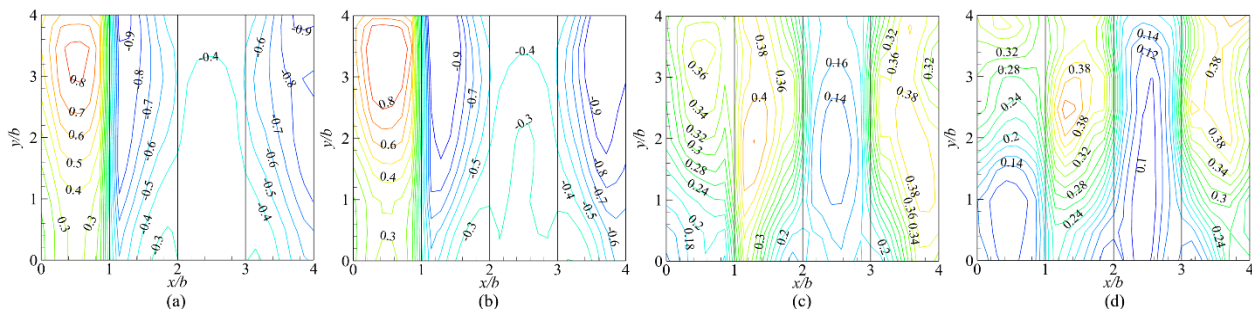


Figure 4. Contour distribution of pressure coefficients. (a) $C_{p_{mean}}$ by experiment, (b) $C_{p_{mean}}$ by ELES, (c) $C_{p_{RMS}}$ by experiment, (d) $C_{p_{RMS}}$ by ELES.